# GRB 160821A: Time varying polarised prompt gamma ray emission

## – Observations and physical modelling

Shabnam Iyyani,[1] Vidushi Sharma,[1] Asaf Pe'er,[2]
and Felix Ryde[3,4]

[1] Inter-University Centre for Astronomy and Astrophysics, Pune, 411007, Maharashtra, India
[2] Department of Physics, Bar-Ilan University, Ramat-Gan, 52900, Israel
[3] Department of Physics, KTH Royal Institute of Technology, AlbaNova, SE-106 91 Stockholm, Sweden
[4] The Oskar Klein Centre for Cosmoparticle Physics, AlbaNova, SE-106 91 Stockholm, Sweden
*E-mail: shabnam@iucaa.in*

Abstract

For the first time, we report a high polarisation fraction of $66^{+26}_{-27}$ % across a gamma ray burst 160821A at $\sim 5.3\sigma$ confidence level. The polarisation angle is found to swing by 80° twice during the burst concurrently with the change in high energy spectrum. The change in polarisation angle is not due to the change in width of the visible part of the jet and thereby rules out axi-symmetric emission models. The high energetics of the burst confirm that the jet is viewed on-axis and therefore, the observed radiation is synchrotron produced in ordered magnetic fields. The standard models of Poynting flux and baryon dominated jets find it difficult to explain these observed features.

Key words: gamma ray burst — GRB160821A — polarisation — synchrotron — non-thermal radiation

## 1. Introduction

Gamma ray bursts (GRB) are the brightest explosions in the universe and lasts only for a few seconds. Despite several decades of study of gamma ray burst, the event largely remains a mystery till date in terms of its jet composition, process of radiation, jet geometry, progenitors etc. Attempts are made to resolve the enigma of radiation process by studying the spectrum of prompt emission. However, currently we face the issue of degeneracy between various spectral models and in such scenarios, we require more constraining observables like polarisation. The measurement of polarisation of prompt gamma ray emission has been an extremely challenging endeavor because of the scarcity of incident photons as well as due to the brevity of the event. Polarisation measurements were reported for only a handful of cases (McConnell 2017; Iyyani 2018). Cadmium Zinc Telluride Imager (CZTI) onboard AstroSat behaves like an open detector for energies above 100 keV and thereby is capable of detecting GRBs. CZTI can measure polarisation of GRBs in $100 - 400$ keV energy range (Chattopadhyay et al. 2019).

In this proceeding, we discuss the results of the spectral and polarimetric analyses done for the GRB 160821A and also the various physical models in this context. GRB 160821A is the third brightest gamma ray burst observed by Fermi gamma ray space telescope till date in terms of its energy flux. It was also the brightest event observed in CZTI during its first two years of its operation.

## 2. Observations

The Fermi Gamma ray Burst Monitor (GBM) triggered at 20:34:30.04 UT and the light curve included a precursor emission starting from trigger time, $T_0$ till $T_0 + 112\,s$ and a bright emission episode with a T90 of $\sim$ 43 s. AstroSat-CZTI also detected the burst and only captured the main episode of the burst with a T90 of 42 s. There was no redshift measurement for the burst. Following the study of host galaxies of long GRBs, and also the constrain of possible isotropic energy, $E_{\gamma,iso}$ for the burst to be $< 10^{56}\,erg$, it is most likely that the redshift of the GRB lies between $z = 0.4$ and $z = 2$. In Table 1, the observed spectral features of the different episodes of the burst: precursor, main episode and afterglow, are summarised.

## 3. Analysis results

The precursor emission was best modelled using a simple cutoff power law function. The emission during

Table 1. In the table below, the important observed features of GRB160821A are summarised.

| Emission episode | Duration [Tstart] | Spectral model | Details |
|---|---|---|---|
| Precursor | 112 s [0 s] | Cutoff power law | a) No quiescent period<br>b) Soft emission in 8 keV - 10 MeV.<br>c) Fluence = $9.72 \pm 0.38 \times 10^{-6}\ erg/cm^2$ |
| Main emission | 86 s [112 s] | Blackbody + Band × Highecut | a) Spectrum deviates from the traditional Band function.<br>c) Fluence = $1.25 \pm 0.03 \times 10^{-3}\ erg/cm^2$ |
| Afterglow | | | |
| LAT ($> 100\,MeV$) | 1847 s [153 s] | Power law | a) LAT flux decays as $F_{LAT}(mJy) \propto t^{-0.49\pm0.13}$<br>b) Spectral power law index $\sim -1.71 \pm 0.51$ |
| Optical (R band) | 4 days [1759 s] | - | c) Optical flux peaks at $t_p = 2124\,s$.<br>d) Optical flux decays in the shallow region as $F_{op}(mJy) \propto t^{-0.55\pm0.001}$.<br>e) A jet break possibly exists between day 1 and 4. |
| Radio (15 GHz) | 10 days [6840 s] | - | f) No Radio detection.<br>Only upper limits are reported. |

the precursor episode amounts to an isotropic energy of $E^{pre}_{\gamma,iso} = 5.4 \pm 0.2 \times 10^{51}\,erg$ ($2.8 \pm 0.1 \times 10^{53}\,erg$) for a redshift, z =0.4 (2).

The time resolved spectral analysis of the main episode of the burst showed significant deviations in the spectrum from the simple phenomenological model "Band function", both at low and high energies. The spectrum was found to be best modelled using a blackbody (BB; $kT \sim 30\,keV$) + Band × Highecut ($f_{BHec}$; Band peak, $E_p \sim 800\,keV$ and high energy cutoff, $E_c \sim 2-50\,MeV$). The evolution of the spectral fit parameters are shown in Figure 4b in Sharma et al. (2019). The low energy part of the spectrum characterised by low energy power law index, $\alpha$ and Band peak, $E_p$ are found to be nearly steady. On the other hand, the high energy part of the spectrum characterised by the high energy power law index, $\beta$ and high energy cutoff, $E_c$ are found to significantly vary such that $\beta$ decreases and $E_c$ increases with time.

A fine time resolved polarisation analysis of the GRB pulse, involving time intervals of $10\,s$ spaced at $2.5\,s$ were conducted. This study showed that polarisation fraction (PF) did not significantly evolve across the pulse, however, the polarisation angle (PA) changed during the rise, peak and decay phases of the pulse. The hardness ratio of Fermi LAT LLE to GBM light curves also showed a change during the pulse. Based on these observations, a broader time resolved polarisation analysis was conducted, thereby dividing the main episode into three main time intervals: 115-129 s, 131 -139 s and 142 -155 s, where these intervals corresponded to the rise, peak and decay phases of the pulse respectively. Polarised emission described by polarisation fractions $71^{+29}_{-41}$ %, $58^{+29}_{-30}$ %, $61^{+39}_{-46}$ % and their respective polarisation angles of $110^{+14}_{-15}{}^\circ$, $31^{+12}_{-10}{}^\circ$, $110^{+25}_{-26}{}^\circ$ were measured in first, second and third time intervals at a statistical significance of 99.8 %, 99.97 % and 99.1 % respectively (Figure 2 in Sharma et al. 2019). A change in polarisation angles by $81^\circ \pm 13^\circ$ during the rise and peak phase of the pulse, and a change by $80^\circ \pm 19^\circ$ during the peak and decay phases of the pulse were observed. A nearly null polarisation was obtained, when the entire pulse, for a time interval 115-155 s was analysed. This measurement can be understood as the result of the intrinsic change in polarisation angles happening within the pulse. Thus, an average polarisation, PF = $66^{+26}_{-27}$ %, across the burst was estimated by taking into account this change in polarisation angle at a statistical significance of $5.3\,\sigma$ (Sharma et al. 2019).

Afterglow data basically includes the extended LAT and the optical emission. We find that the LAT emission satisfies the closure relation [1] for the case of slow cooling synchrotron emission produced in external shock occuring in a uniform circumstellar medium. The emission corresponds to the synchrotron spectral regime $\nu_m < \nu < \nu_c$, where $\chi$ should be $(p-1)/2$, where $p$ is the power law index of the electron distribution, which is found to be $2.42 \pm 1.02$. This spectral regime cools adiabatically with time such that $F_\nu \propto t^{-3(p-1)/4}$. For the obtained $p$ value, we find the expected $\phi_{exp} = 1.07 \pm 0.77$, which is consistent within errors of the observed temporal evolution, of $\phi = 0.496 \pm 0.127$ (see Table 1). Thus using the equation for $\nu F_\nu$ of slow cooling synchrotron emission in the case of adiabatic evolution of the shock, given in Racusin et al. 2011, we estimate the kinetic energy of the burst to be $E_k = 6.4 \times 10^{53}$ ($5.5 \times 10^{54}$) erg for a redshift z=0.4 (2). The radiative efficiency of the burst is found to be $\kappa = 0.52\,(0.87)$. Relating the possible break in the decay of optical flux between day 1 and 4 to as the jet break, we estimate the jet opening angle to be between $5-8\,(2.5-4)$ for redshift z=0.4 (2). The optical flux is found to peak at $t_p = 2124\,s$. This peak time can be related to the deceleration timescale where the Lorentz factor of the jet reduces to half its initial value. For a uniform ambient medium, the initial

*1 general convention is $F_\nu \propto t^{-\phi}\,\nu^{-\chi}$

Lorentz factor of the jet, $\Gamma$, as it crashes into the ambient medium is found to be 128 (262).

## 4. Discussion: Physical modelling

Any proposed physical model has to explain the following observed features: (i) very high energetics ($E_{\gamma,iso} > 10^{53}$ erg); (ii) high radiation efficiency ($> 50\%$); (iii) non-zero and high polarisation ($PF > 30\%$); (iv) swing in polarisation angle on timescales of $\sim 10\,s$; (v) the concurrent change in high energy spectrum and (vi) the weak preceding emission of $\sim 100\,s$.

Photospheric emission models can explain high radiation efficiency, it can produce spectrum with multiple breaks by taking into account sub-photospheric dissipation and also can produce polarisation up to $\sim 40\%$ in the scenario when a narrow jet is viewed off-axis (Lundman et al. 2014). However, the high energetics of the burst suggest that the jet is pointed towards the observer. In photospheric emission models, a change in PA by 90° is expected when there is a change in the width of the visible part of the jet and this can happen due to the change in the velocity field distribution attributed to the central engine. In such a change, when the visible width of the jet increases, the PF is expected to decrease (PF $< 10\%$) which, however, is not observed in 160821A.

From Figure 1, we can see that when viewed on-axis, the high PF is expected only in case of synchrotron emission produced in magnetic fields which are ordered on angular scales of $1/\Gamma$ and axisymmetric emission models, like inverse Compton scattering or synchrotron emission produced in random magnetic fields like those expected in internal shocks are thereby ruled out. In Poynting flux dominated scenarios, the magnetic reconnections are considered to be the mechanism of dissipating the magnetic energy of the jet, which is eventually radiated away by the energised electrons. At reconnection site, the magnetic fields are generally expected to get randomised, in such a scenario, the change in PA is expected to be random. On the other hand, if we assume that at least a fraction of the field lines still remain ordered on angular scales of $1/\Gamma$ after magnetic reconnections, even then as discussed above the possible change in width of the visible part of the jet cannot account for the observed change in PA. In yet another scenario, we can envisage a Poynting flux dominated jet with a dominant toroidal component of magnetic fields at the dissipation site results in synchrotron radiation which results in the broad emission pulse constituting the NaI light curves. At some later time, a blob of magnetized plasma with a different magnetic orientation is ejected from the central engine whose synchrotron emission now dominates and produces the narrow emission pulse seen in the LLE light curve. The observed emission is, thus, due to the synchrotron radiation produced in ordered magnetic fields

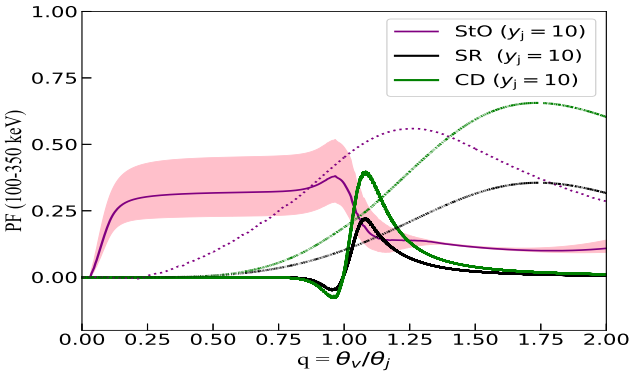


Fig. 1. The PF expected for different emission processes like synchrotron emission in a toroidal magnetic field (StO, purple), synchrotron emission in random magnetic fields (SR, black) and Compton drag (CD, green) with respect to $q = \theta_v/\theta_j$ for $y_j = 10$ (solid line) and 1 (dotted and shaded line) are shown. In the above models, the polarisation estimations are done for a power law spectrum with $\alpha = -0.97$ (the average $\alpha$ across the main episode). The upper and lower bounds of the pink shaded region represents the PF expected from the fast and slow cooling synchrotron emission in a toroidal magnetic field for $y_j = 10$. These bounds are also consistent with the lowest and highest $\alpha$ observed during the main episode.

but with different orientations in these regions. This can explain the high linear polarization and depending on the dominance of these emissions, a change in polarization angle happens with time. In this scenario, due to different microphysical parameters possible at the different emission regions, we would expect to see some change in the low energy part of the spectrum which constitutes the peak of the spectrum. However, here we observe a nearly steady low energy spectrum which is quite intriguing.

Thus, GRB160821A has been an exceptional burst in terms of its spectrum as well as polarisation measurements which are highly constraining. We find that the standard models of both Poynting flux as well as baryon dominated outflow cannot easily explain the observations.

## References


McConnell, M. L. 2017, New Astr. Rev., 76, 1

Iyyani, S. 2018, JAA, 39, 75

Chattopadhyay, T., Vadawale, S., Aarthy, E., et al. 2019, ApJ, 884, 123

Sharma, V., Iyyani, S., Bhattacharya, D., et al. 2019, ApJL, 882, L10

Racusin, J. L., Oates, S. R., Schady, P. , et al. 2011, ApJ, 738, 138

Lundman, C. and Pe'er, A. and Ryde, F., et al. 2014, MNRAS, 440, 3292